JOURNAL OF CATALYSIS 155, 390–402 (1995)

Oxidative Coupling of Methane over Oxide-Supported Sodium–Manganese Catalysts

Dingjun Wang, Michael P. Rosynek, and Jack H. Lunsford[1]

Department of Chemistry, Texas A & M University, College Station, Texas 77843

Received December 28, 1994; revised April 28, 1995

The oxidative coupling of methane over $Mn/Na_2WO_4/SiO_2$, $Mn/Na_2WO_4/MgO$, and $NaMnO_4/MgO$ catalysts was studied using both a cofeed flow system and a pulse reactor. At 800°C and 1 atm, and using a CH_4/O_2 ratio of *ca.* 8/1, a methane conversion of 20% was achieved at a C_{2+} selectivity of ≥80%, with no diluent in the reagents. The similar catalytic behaviors of the three catalysts suggest that a common active site, consisting of an Na–O–Mn species, may be involved. Results from a pulse reaction sequence (an O_2 pulse followed by a series of pure CH_4 pulses) indicate that the active species are not stable under reaction conditions unless gas phase O_2 is present, and that bulk lattice oxygen does not participate in the methane coupling reaction when carried out in the cofeed mode. There is a linear relationship between the specific activity for CH_4 conversion and the concentration of surface Mn, which is believed to be responsible for the activation of O_2. The resulting form of oxygen then abstracts a hydrogen atom from CH_4. Sodium is essential for preventing the complete oxidation of CH_4, perhaps by isolating the Mn ions. The tungstate ions appear to impart stability to the catalysts. © 1995 Academic Press, Inc.

INTRODUCTION

The partial oxidation of methane with molecular oxygen to produce C_{2+} hydrocarbons has been the subject of intense research during the past decade. A wide variety of oxide catalysts has been studied for the oxidative coupling of methane (OCM), and these have recently been reviewed (1–3). However, only a few of the many catalysts studied can achieve C_{2+} selectivities of at least 80% at CH_4 conversion levels >15% for long periods (4–10). Sodium-promoted manganese oxides are among the most promising catalysts reported thus far, in terms of stability and productivity (7, 8). Similar catalytic performances were observed over several different supported manganese oxide catalysts, and a common redox mechanism involving lattice oxygen has been proposed (7, 8). Nevertheless, there remains considerable disagreement concerning the nature of the active phases, the role of promoters, and the nature of the active oxygen species in the catalysts.

Sofranko and co-workers (10) postulated that the species responsible for selective oxidation on these catalysts may be a manganese silicate or manganese oxide perturbed by a strong support interaction. It is believed that the addition of Na^+ ions decreases the surface area and increases the surface basicity of the catalyst, while the pyrophosphate anion, which is a component of some of the catalysts, provides greater stability (11). It was found that the $Mn/Na_4P_2O_7/SiO_2$ and $NaMnO_4/MgO$ catalysts were active and selective in both the cofeed and cyclic modes, although the C_{2+} yields were not greater in the cyclic mode (7). Based on XRD data and the results of ^{18}O exchange experiments, Labinger *et al.* (12) proposed that the active species in the $NaMnO_4/MgO$ catalyst is composed of ordered domains of Mg_6MnO_8 in MgO. Burch *et al.* (13), who investigated a series of K-promoted Mn oxide catalysts using XPS and XRD, suggested that the active and selective species was associated with a Mn_3O_4-like phase. Similarly, Moggridge *et al.* (14) carried out *in situ* XRD studies of modified manganese oxide catalysts, and concluded that a KCl-promoted Mn_3O_4 phase, which was formed upon injection of $CHCl_3$ into the KCl/MnO_2 system, was responsible for the high C_2 selectivity. Recently, a group of Chinese researchers found that a stable catalyst, comprising 1.9 wt% Mn/5% Na_2WO_4/SiO_2, was very active and selective for the formation of C_{2+} products in methane oxidative coupling (8). The authors proposed that a surface W species containing W=O and three W–O–Si bonds is responsible for the oxidative coupling of methane; whereas, manganese oxide, present as Mn_2O_3 in the catalyst, only enhances exchange between gas-phase oxygen and lattice oxygen and promotes lattice oxygen transport (15).

Operation of OCM catalysts in the cyclic mode supports the postulate that, in many cases, bulk lattice oxygen participates in the coupling reaction (10, 11, 16–18). For example, Keller and Bhasin estimated that the oxidation–reduction cycle involved 10–20 atomic layers near the surface, suggesting that lattice oxide ions (i.e., O^{2-}) are involved in

[1] To whom correspondence should be addressed.

0021-9517/95 $12.00
Copyright © 1995 by Academic Press, Inc.
All rights of reproduction in any form reserved.

the reaction (16). Sofranko *et al.* (7) proposed that the same mechanism can be used to explain the catalytic chemistry over a $Mn/Na_4P_2O_7/SiO_2$ catalyst in both the cyclic and the cofeed modes; that is, methane is first oxidized to methyl radicals by the lattice oxygen species, and the resulting reduced metal oxides are subsequently reoxidized in a separate regeneration step. Recently, a redox mechanism involving lattice oxygen ions and the W^{6+}/W^{5+} ion pair was also proposed for the OCM reaction over a $Mn/Na_2WO_4/SiO_2$ catalyst in the cofeed mode (8).

Otsuka *et al.* (17–19), who investigated the roles of lattice oxygen in methane activation over $LiNiO_2$ and LiCl/NiO catalysts, concluded that lattice oxygen ions in the $LiNiO_2$ catalyst are responsible for the activation of methane; however, over the LiCl/NiO catalyst, the active oxygen species are believed to be in the form of adsorbed oxygen in the presence of gaseous oxygen. As a result of transient experiments involving step, pulse, and steady-state isotopic switches, Wolf and co-workers (20) concluded that there was little involvement of lattice oxygen during the OCM reaction over $Na/NiTiO_3$; on a $Li/NiTiO_3$ catalyst, by contrast, the activity was mainly due to lattice oxygen participation.

In the present study, the catalytic performances of $Mn/Na_2WO_4/SiO_2$, $Mn/Na_2WO_4/MgO$, and $NaMnO_4/MgO$ catalysts were evaluated in both a continuous flow reactor and a pulse mode. The roles of the various catalyst components were established by correlating the catalytic results with both bulk and surface properties of the catalysts. The temporal results of pulse reactions provided information concerning the possible role of bulk lattice oxygen and adsorbed oxygen in the selective oxidation reactions.

EXPERIMENTAL

Catalysts. The SiO_2-supported catalysts were prepared by incipient wetness impregnation, at 85°C, of a silica gel support (Davison, 57-08-5) with aqueous solutions having appropriate concentrations of $Mn(NO_3)_3$ and Na_2WO_4. The catalysts were then dried for 4–8 h at 130°C and calcined for 8 h at 800°C. The MgO-supported catalysts were prepared by slurrying MgO (Fisher "light", M-349-4, 98% pure) with H_2O at 85°C in a 500-ml, 3-neck round-bottomed flask, equipped with an addition funnel and a water-cooled condenser. $Mn(NO_3)_2$ and Na_2WO_4 were added to the slurry during a 1 h period while maintaining the same temperature for an additional 5 h. The resulting slurry was then dried for 4–5 h at 130°C and calcined for 8 h at 800°C. $NaMnO_4/MgO$ catalysts were prepared by slurrying MgO with a solution of $NaMnO_4$, and then calcining for 16 h at 900°C. All of the dried catalyst samples were crushed and sieved to 20/45 mesh size; in all subsequent references, the amounts of the various components are expressed in weight percent.

Reactor systems. Reactions were carried out in both a cofeed flow system and a pulse mode, using reactors constructed from alumina tubes (Coors, AD-998, 99.8% Al_2O_3). The flow reactor had an i.d. of 6.4 mm, and the volume of the catalyst used was 1.0 ml, unless otherwise specified. The microreactor used to perform pulse reaction studies had an i.d. of 4.5 mm, and approximately 0.15 ml (0.05–0.13 g) of catalyst was used in each case. To minimize the contribution from any gas-phase reactions, quartz chips filled the space above and below the catalyst beds in both the flow and the pulse reactors. A thermocouple in a smaller alumina tube was attached to the outside wall of each of the reactors.

Reactant gases, which included CH_4 (99.9%), O_2 (99.95%), He (99.999%), and CO_2 (99.5%), were obtained from Matheson and were used without further purification. Gas flows were regulated by mass flow controllers (MKS Model 1159A). In the flow system, the catalyst was heated in a flow of O_2 to 800°C before admission of reaction gases. At the reactor outlet, two traps cooled to 0°C were used to remove most of the water from the exit gas stream. The reaction mixtures were then analyzed by gas chromatography (HP5890A), using a Spherocarb column. All studies, unless otherwise stated, were carried out at atmospheric pressure, without diluting the reagents with an inert gas. For the pulse-flow system, He was used as the carrier gas, at a flow rate of 44 ml/min. The reactor was first heated to 800°C in a flow of O_2 and then in a flow of He for 30 min before beginning to inject reactant pulses. The reaction mixtures were analyzed using a gas chromatograph (Carle) equipped with a Porapak-R column.

Catalyst characterization. Inductively coupled plasma (ICP) spectroscopy was used to analyze the bulk compositions of the catalysts. X-ray diffraction (XRD), using a Seifert-Scintag PAD V diffractometer, was employed to determine the bulk crystalline phases of fresh catalysts.

XPS and ISS spectra, which were used to determine the abundance and chemical state of surface components of the catalysts, were acquired using a Perkin–Elmer (PHI) Model 5500 spectrometer. All spectra were obtained using samples prepared in the form of pressed wafers and treated in one of two ways: (i) "fresh" samples were prepared by treating the previously calcined samples in a separate quartz reactor system in a stream of O_2 at 800°C for 6–12 h, and (ii) "used" samples were prepared by treating the fresh catalysts in a $CH_4:O_2$ reaction mixture at 800°C for a certain time, duplicating those employed in the catalytic reaction experiments. The quartz reactor system used for these treatments allowed *in situ* transfer of the ceramic holder containing the treated sample into an O-ring-sealed stainless steel transport vessel. The removable vessel was then transferred to the inlet system of the XPS spectrometer, and the sample was introduced into the UHV analysis

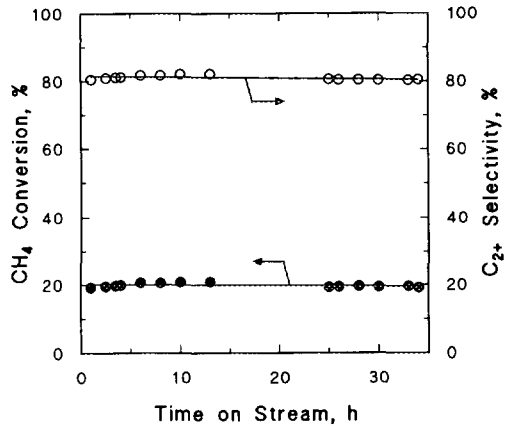

FIG. 1. Oxidative coupling of methane as a function of time on stream over 2% Mn/5% Na_2WO_4/MgO (T = 800°C, CH_4/O_2 = 670/90 Torr, total flow rate = 115 ml/min, 1.0 ml catalyst).

chamber of the instrument without exposure to the air. In a typical XPS data acquisition, a pass energy of 29.3 eV, a step increment of 0.125 eV, and an Mg anode power of 400 W were employed. All binding energies were referenced to the C 1*s* line of adventitious carbon at 284.6 eV. In cases where the amount of adventitious carbon was too small to provide an accurate reference, the binding energy was referenced to the Au $4f_{7/2}$ peak at 83.8 eV, resulting from prior deposition of a small gold spot onto the sample. Near-surface compositions were calculated from peak areas using sensitivity factors that are provided in the software of the instrument. Stoichiometries were measured for several pure samples that contained the relevant elements, and the values obtained were within 10 to 20% of those expected from the bulk composition. For example, the near-surface O/Si ratio in SiO_2 was 2.0 and the Na/W/O ratio in Na_2WO_4 was 2:1.1:4.4. ISS spectra were obtained using $^3He^+$ ions at a scattering angle of 134.5° and ~1 kV accelerating potential.

RESULTS AND DISCUSSION

Catalytic Reaction Results

Flow reactor studies. As shown in Fig. 1, a CH_4 conversion of 20% and a C_{2+} selectivity of 80%, with a C_2H_4/C_2H_6 product ratio of 1.3, were achieved over a 2% Mn/5% Na_2WO_4/MgO catalyst at 800°C using a CH_4/O_2 reactant ratio of 7.4, with no dilution of the reagent gas. Moreover, these levels could be sustained unchanged for more than 30 h of time on stream. This is the best overall catalyst performance that has yet been reported for methane coupling in the cofeed mode.

It is particularly noteworthy that virtually identical results were obtained over a catalyst having the same Mn/Na_2WO_4 composition, but with SiO_2 substituted for MgO, as shown in Fig. 2a. This is essentially the same catalyst as that reported by the Chinese group (8), although their results were obtained under different conditions. Similarly, the *initial* activity and selectivity behavior of the $NaMnO_4$/MgO catalyst (Fig. 2b), which contained no W, closely resembled that of the corresponding Mn/Na_2WO_4/MgO catalyst. Although these data were obtained under oxygen-limited conditions, the nearly identical behaviors suggest that the catalytically active species may be the same in all three catalysts, and, furthermore, that W may not be a necessary component of this active species. However, close inspection of the data in Fig. 2b for the $NaMnO_4$/MgO catalyst reveals that the methane conversion gradually decreased with increasing time on stream. After 20 h on stream (not shown in Fig. 2b), the decrease in conversion became even more apparent. Thus, it appears that tungsten plays a role in stabilizing the catalyst, perhaps by preventing loss of sodium. A similar effect was observed over a Mn/$Na_4P_2O_7/SiO_2$ catalyst in which $P_2O_7^{4+}$ ions were believed to prevent catalyst deactivation (11).

The need for the stabilizing effect of W is even more apparent in the case of $NaMnO_4/SiO_2$ (Fig. 2c), for which even the initial activity and selectivity are inferior to those of its tungsten-containing counterpart (Fig. 2a). As will be shown below, the surface concentration of sodium decreased significantly during OCM reaction on the 5% $NaMnO_4$/MgO catalyst, while the sodium content on the surface of the 2% Mn/5% Na_2WO_4/MgO catalyst appeared relatively stable. XRD results indicate that the presence of WO_4^{2+} ions in the SiO_2-supported catalyst prevents the formation of sodium and manganese silicates.

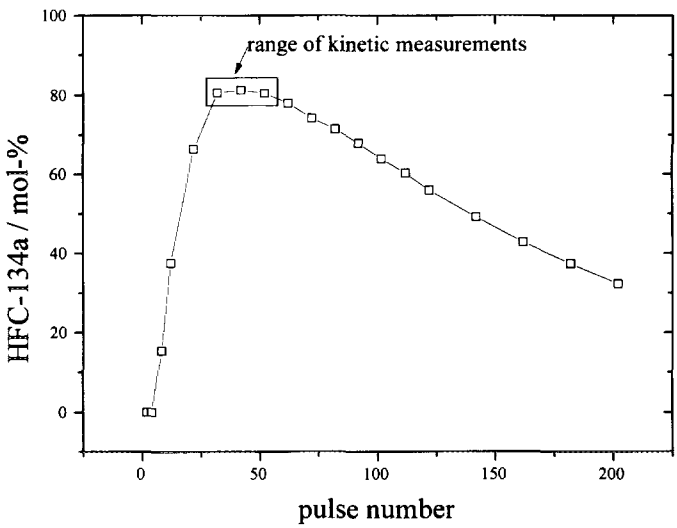

FIG. 2. Oxidative coupling of methane as a function of time on stream (T = 800°C, CH_4/O_2 = 670/90 Torr, total flow rate = 115 ml/min, 1.0 ml catalyst). Conversion and selectivity over: (a) 2% Mn/5% Na_2WO_4/SiO_2; (b) 5% $NaMnO_4$/MgO; (c) 5% $NaMnO_4/SiO_2$; (d) 5% Na_2WO_4/MgO.

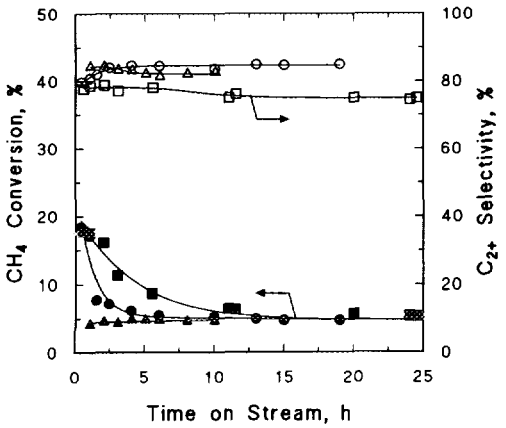

FIG. 3. Oxidative coupling of methane as a function of time on stream under differential conditions (T = 800°C, CH_4/O_2 = 670/90 Torr, total flow rate = 115 ml/min, 0.3 ml catalyst). ●, ○, 2% Mn/5% Na_2WO_4/SiO_2; ■, □, 2% Mn/5% Na_2WO_4/MgO; ▲, △, 5% $NaMnO_4$/MgO.

TABLE 1

Bulk Compositions and Surface Areas of Selected Catalysts

Catalyst	Condition	Bulk content (wt%)[a] Na	W	Mn	Surface area (m^2/g)
2% Mn/5% Na_2WO_4/MgO	Fresh[b]	0.9	3.4	2.0	23
	Used[c]	0.7	3.3	2.1	8
2% Mn/5% Na_2WO_4/SiO_2	Fresh[b]	0.9	3.5	2.4	2.5
	Used[c]	nd	nd	nd	0.8
5% $NaMnO_4$/MgO	Fresh[b]	0.8	—	1.9	1.7
	Used[c]	0.5	—	1.5	1.5

Note. The letters "nd" denote that no data is available.

[a] Based on ICP analyses.

[b] After treatment in flowing O_2 for 8 h at 800°C.

[c] After exposure to CH_4/O_2 = 670/90 Torr reaction mixture (115 ml/min) for 24 h at 800°C.

As shown in Fig. 2d for 5% Na_2WO_4/MgO, the absence of Mn results in a poor methane oxidation catalyst, indicating that Mn is an essential component of the active phase in these catalysts. A similar inferior performance was observed over 5% Na_2WO_4/SiO_2 (not shown in Fig. 2). These results are inconsistent with the proposal by Li and coworkers (8, 15) that the active sites in the Mn/Na_2WO_4/SiO_2 catalyst consist of a Si–O–W species, since neither Si nor W is a necessary component of an active catalyst (compare the results of Figs. 1 and 2b), and with the suggestion of Labinger *et al.* (12) that a Mg_6MnO_8 phase may play an important role in the formation of the active phase, since Mg is similarly not essential (Fig. 2a).

Under differential reaction conditions (i.e., at sufficiently low CH_4 conversions such that O_2 was not limiting), the steady-state behaviors of all three of the Mn-containing catalysts were comparable (Fig. 3). Although the methane conversion declined from 18 to 5% after 10 h on stream over the 2% Mn/5% Na_2WO_4/MgO and 2% Mn/5% Na_2WO_4/MgO catalysts, these deactivations can be attributed to corresponding decreases in the surface areas of these two catalysts. As shown in Table 1, the surface areas of both catalysts decreased to approximately one-third of their initial values after 22–26 h on stream. It should be noted that the rate at which each catalyst sinters depends on the space velocity; the catalysts lost surface area more rapidly under differential reaction conditions. These initial deactivations may be prevented by precalcining the catalysts at 900°C. For example, the $NaMnO_4$/MgO catalyst, when calcined at 900°C for 16 h, displayed a stable, albeit lower, activity (Fig. 3). The somewhat lower C_{2+} selectivity observed for the Mn/Na_2WO_4/MgO catalyst may reflect the fact that this catalyst has a much larger surface area than those of the other two (Table 1).

In order to obtain additional information about the comparative importance of the various catalyst components, as well as the origin and nature of the active species on these materials, several MgO- and SiO_2-supported catalysts having various nominal bulk compositions were synthesized, and their activities and selectivities for methane coupling under integral conditions (i.e., O_2-limited conditions) at 800°C were examined. As shown in Fig. 4a, Na_2WO_4/MgO containing no Mn exhibited a CH_4 conversion and a C_{2+} selectivity of only 3.6 and 58%, respectively. The overall catalytic performance improved significantly upon the addition of even very small amounts of Mn, and attained its maximum level of ~20% CH_4 conversion and >80% C_{2+} selectivity at an Mn level of only 1%, above which no additional improvement in catalytic performance occurred. Similarly, Mn/MgO (prepared from $Mn(NO_3)_2$, not from $NaMnO_4$) displayed inferior catalytic behavior (Fig. 4b), but its performance improved markedly upon addition of Na (as Na_2WO_4), up to a Na_2WO_4 content of 5 wt%. These results, together with the fact that $NaMnO_4$/

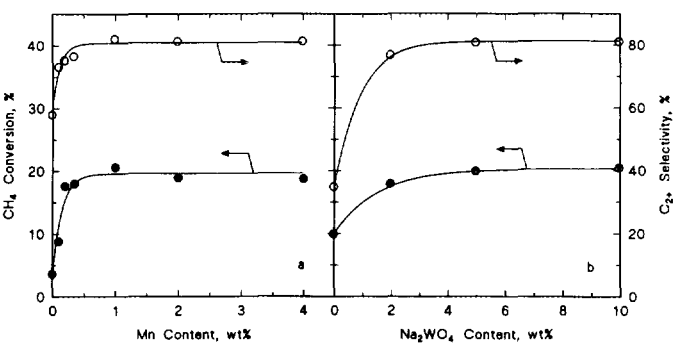

FIG. 4. CH_4 conversion and C_{2+} selectivity as a function of: (a) Mn content; (b) Na_2WO_4 content. (T = 800°C, CH_4/O_2 = 670/90 Torr, total flow rate = 115 ml/min, 1.0 ml catalyst.)

MgO (containing no Na_2WO_4) is a good catalyst, suggest that Na^+ is also an essential component of the active sites.

The role of sodium was investigated further by determining the effects of alternative sources of Na^+ in the catalyst preparations. The presence of Na^+ in the form of carbonates, for example, did *not* improve the performances of the $Mn/Na_2WO_4/MgO$ and $Mn/Na_2WO_4/SiO_2$ catalysts. Addition of 2 wt% or 4 wt% of Na_2CO_3 to the 2% Mn/5% Na_2WO_4/MgO catalyst caused a decrease in conversion from 20% to 18% and 16%, respectively, while the selectivity also decreased slightly. Several factors, including a decrease in surface area, may be responsible for the decrease in C_{2+} yield. A similar inferior performance was observed for the $Na_2CO_3/Mn/Na_2WO_4/SiO_2$ system. Several additional MgO-supported catalysts, with varying Na/Mn ratios, were prepared from Na_2CO_3 and $Mn(NO_3)_2$. It was observed that those having Na/Mn ratios of 1 to 2 displayed catalytic behaviors identical to those synthesized from $NaMnO_4$, whereas the catalysts having Na/Mn ratios <0.5 exhibited much poorer activity and selectivity under oxygen-limiting conditions. These results further demonstrate that manganese ions and sodium ions, rather than tungsten ions, are involved in the formation of the active species. When Na ions were replaced by K ions in a 5% $KMnO_4$/MgO catalyst, a CH_4 conversion of 17% was achieved at a C_{2+} selectivity of 74% under the same reaction conditions.

The 2% Mn/5% Na_2WO_4/SiO_2 catalyst had a much greater *specific* activity for CH_4 conversion (5.3 μmol/s/m^2) than did the 2% Mn/5% Na_2WO_4/MgO catalyst (0.8 μmol/s/m^2), while the $NaMnO_4$/MgO catalyst displayed an intermediate activity (2.4 μmol/s/m^2), based on the total surface areas of the used catalysts. However, the actual activities, of course, depend on the surface densities of the active sites. As will be shown below, the concentrations of Mn in the near-surface regions of the 2% Mn/5% Na_2WO_4/SiO_2, 5% $NaMnO_4$/MgO, and 2% Mn/5% Na_2WO_4/MgO catalysts were 5.0, 2.2, and 0.84 mol%, respectively, following the catalytic reaction, and correlate closely with the observed specific activities. Therefore, it is apparent that the higher surface concentration of manganese in the 2% Mn/5% Na_2WO_4/SiO_2 catalyst is responsible for its higher specific activity. This relationship between manganese concentration and specific activity strongly suggests that Mn ions are directly involved in the formation of the active species.

Thus, it appears that the active phase for the Mn/Na_2WO_4 catalysts is not $Na_2CO_3/Na_2O_2/Na_2O$, which has been suggested for Na_2CO_3/Ln_xO_y catalysts (21). In the latter case, it was found that those lanthanide oxides which contain multivalent cations, and which are responsible for catalyzing nonselective oxidation reactions, were completely covered by a $Na_2CO_3/Na_2O_2/Na_2O$ phase (22). However, as will be shown below by the ISS results, Mn ions and W ions, which also have multiple oxidation states,

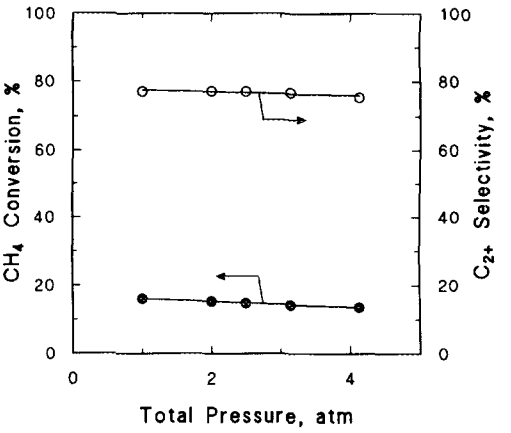

FIG. 5. Effect of total reaction pressure on oxidative coupling of methane over 2% Mn/5% Na_2WO_4/SiO_2. (T = 785°C, $P(CH_4)/P(O_2)$ = 10, 0.1 g (0.22 ml) catalyst, contact time = 0.13 s.)

were observed in the surface layers of the Mn/Na_2WO_4/MgO and $Mn/Na_2WO_4/SiO_2$ catalysts. It is apparent that a different kind of active center, consisting of an Mn–Na–O species is responsible for the high activity and selectivity of the OCM reaction over these catalysts.

For commercial applications, the OCM reaction would preferably be carried out at an elevated pressure. As shown in Fig. 5, under conditions of constant space velocity (250 ml/min/g at the pressure of the experiment) and at a reaction temperature of 785°C with a $P(CH_4)/P(O_2)$ ratio of 10, both CH_4 conversion and C_{2+} selectivity decreased only slightly with increasing reactant pressure over the $Mn/Na_2WO_4/SiO_2$ catalyst, indicating that this catalyst can be effectively used at elevated pressures. It should be noted that at 1 atm pressure the conversion shown in Fig. 5 was less than that in Fig. 2a because the reaction conditions were different. At 800°C and at a flow rate of 550 ml/min over 1 ml of catalyst, a methane conversion of 13–14%, with a C_{2+} selectivity of 80%, was attained at a pressure of 5 atm, and was maintained for a period of 60 h. This is one of the few reported examples of favorable oxidative coupling behavior being achieved at such high pressures. Pinabian-Carlier *et al.* (25) observed a CH_4 conversion of 13% and a C_{2+} selectivity of 80% at 3 atm over a Sr/La_2O_3 catalyst.

Pulse reaction studies. As noted previously, Sofranko *et al.* (10) have demonstrated that alkali- and alkaline-earth-promoted Mn/SiO_2 catalysts for the OCM reaction can function effectively in the so-called redox mode of operation, in which the reactant feed stream is periodically alternated between pure CH_4 and pure O_2. In this technique, the CH_4 undergoes oxidation due to the participation of lattice oxygen species, which are replenished when the reactant stream is subsequently switched to pure O_2

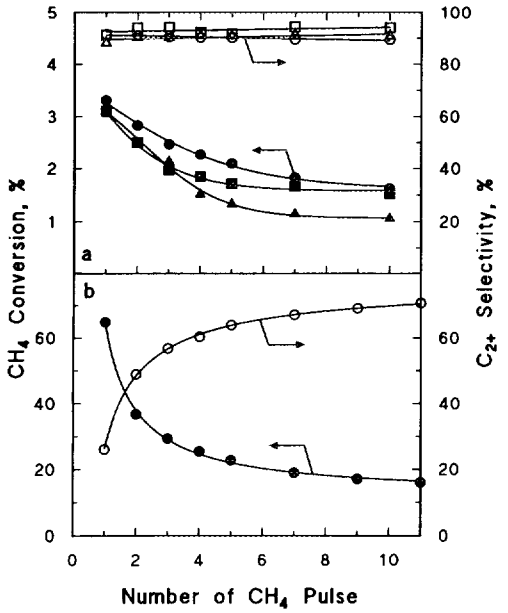

FIG. 6. Variation in CH_4 conversion and C_{2+} selectivity with successive CH_4 pulses at T = 800°C, $P(CH_4)/P(O_2)$ = 5, carrier gas flow rate = 45 ml/min. (a) ●, ○, 2% Mn/5% Na_2WO_4/SiO_2 (0.15 ml); ■, □, 2% Mn/5% Na_2WO_4/MgO (0.15 ml); ▲, △, 5% $NaMnO_4$/MgO (0.15 ml). (b) 12.5% $NaMnO_4$/MgO (2.0 ml).

or air. This approach is in contrast to the more commonly employed cofeed mode of operation, in which the reactant stream contains both CH_4 and O_2. In order to determine the extent of lattice oxygen involvement in the case of the present Mn-containing catalysts, we have performed a series of pulse reaction experiments. Figure 6a shows CH_4 conversions and C_{2+} selectivities observed at 800°C for a succession of CH_4 pulses over previously oxidized samples of 2% Mn/5% Na_2WO_4/SiO_2, 5% $NaMnO_4$/MgO, and 2% Mn/5% Na_2WO_4/MgO catalysts. The gas hourly space velocities (GHSV) approximated those employed in the previously described cofeed studies over these catalysts (Fig. 2). Although C_{2+} selectivities were high for all three catalysts, the CH_4 conversion levels (1 to 3%) obtained with these O_2-free pulses were significantly inferior to those (~20%) observed in the cofeed mode of operation with these catalysts. However, when the GHSV over a 12.5% $NaMnO_4$/MgO catalyst was decreased (by increasing the amount of catalyst employed) to a range comparable to that employed by Sofranko *et al.*, the resulting catalytic performance (Fig. 6b) after several CH_4 pulses more closely resembled the results obtained in the cofeed mode. Moreover, the conversion and selectivity agreed with those reported by Sofranko *et al.* (7). These results indicate that bulk lattice oxygen plays little or no role during the methane oxidative coupling reaction over these catalysts in the cofeed mode. Although it is not generally appreciated, Sofranko *et al.* (7) previously pointed out that their catalysts were much more active in the cofeed mode than in the redox mode.

To further demonstrate the importance of gas-phase oxygen in maintaining high conversion levels with these catalysts, additional pulse reaction studies were performed in which a pulse of pure O_2 was followed by one of pure CH_4 over 2% Mn/5% Na_2WO_4/SiO_2, 5% $NaMnO_4$/MgO, and 2% Mn/MgO catalysts, with increasing time intervals between the two pulses. The results are presented in Fig. 7, where the first data point, corresponding to zero time between O_2 and CH_4 pulses, was obtained using a pulse that contained premixed reactants (CH_4/O_2 = 5). When the time interval between the initial O_2 pulse and the subsequent CH_4 pulse was as little as one second, the conversion of methane over the 2% Mn/5% Na_2WO_4/SiO_2 catalyst decreased dramatically from about 18% for the cofeed pulse to <5% (Fig. 7a). When the delay between O_2 and CH_4 pulses was five seconds or longer, the conversion decreased to <2%, which is comparable to that observed without intervening O_2 pulses (Fig. 6a). Similar results were obtained over the 5% $NaMnO_4$/MgO catalyst (Fig. 7a) and over the 2% Mn/5% Na_2WO_4/MgO catalyst (results not shown), which further suggests that the active site is the same for all three catalysts. In the case of the 2% Mn/MgO catalyst, which contained no Na, the C_{2+} selectivity was only ~20% (Fig. 7b), while the methane conversion declined in the same manner as that observed for the sodium-promoted manganese catalysts (Fig. 7a). It is apparent from these results that the presence of gas-phase oxy-

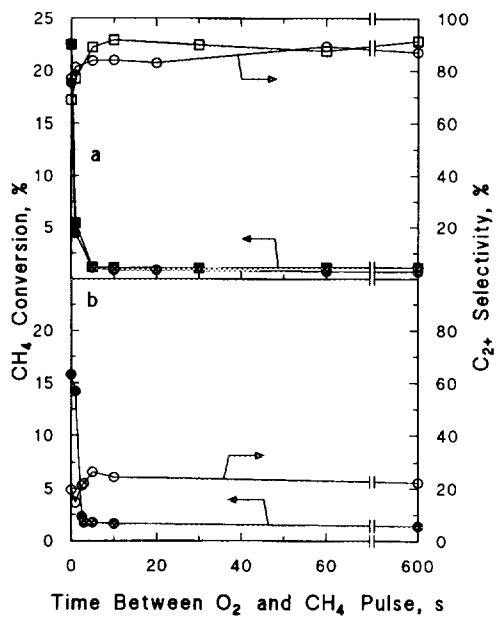

FIG. 7. Effect of delay time between O_2 and CH_4 pulses on the oxidative coupling of methane at T = 800°C, $P(CH_4)/P(O_2)$ = 5, carrier gas flow rate = 45 ml/min, and 0.15 ml catalyst. (a) ●, ○, 2% Mn/5% Na_2WO_4/SiO_2; ■, □, 5% $NaMnO_4$/MgO. (b) ●, ○, 2% Mn/MgO.

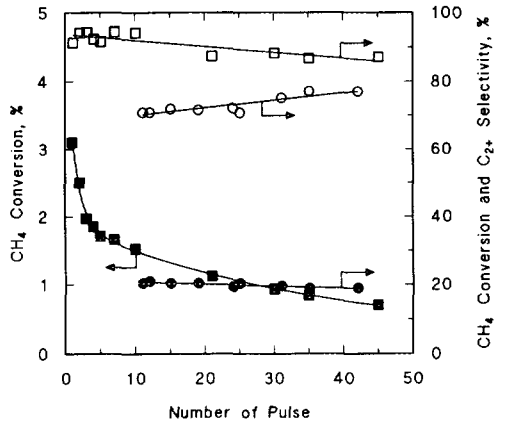

FIG. 8. Oxidative coupling of methane over 2% Mn/5% Na_2WO_4/SiO_2 as a function of the number of CH_4 or premixed CH_4/O_2 pulses at T = 800°C, carrier gas flow rate = 45 ml/min, and 0.15 ml catalyst. ●, ○, premixed $P(CH_4)/P(O_2)$ pulse; ■, □, pure CH_4 pulse. The catalyst was recalcined in O_2 at 800°C for 1 h after every 10th pulse.

gen is necessary to achieve high CH_4 conversion with all of these catalysts, and that bulk lattice oxygen contributes little to the activity. The data also demonstrate that the active sites, either selective or nonselective, may be created by interaction between gas-phase oxygen and surface manganese ions. The active species has a very short lifetime, e.g., less than one second. Sodium ions significantly improve the C_{2+} selectivity, but not the activity.

The pulse reaction data presented in Fig. 6a indicate that CH_4 conversions are low, even for the *first* CH_4 pulse, over the previously oxidized catalysts. Moreover, the activities continue to decline with each successive CH_4 pulse. In order to determine the extent of reversibility of this deactivation for the $Mn/Na_2WO_4/SiO_2$ catalyst, the pulse reaction experiments depicted in Fig. 8 were performed over an extended period. Here, the circles represent results obtained using premixed (i.e., cofeed) pulses, in which CH_4/O_2 = 5, and the squares are results for pure CH_4 pulses. In the latter case, the catalyst was initially treated in flowing O_2 for 1 h at 800°C and then flushed with He at the same temperature for 10 min prior to exposure to the first CH_4 pulse. During the course of the extended experiment, the catalyst was again periodically treated in O_2 under the same conditions after every 10th pulse of CH_4. It should be noted that the cofed pulses were interspersed between the pure CH_4 pulses. Methane conversions for the cofed pulses are shown on the right-hand ordinate scale, while those for the pure CH_4 pulses are given on the left-hand ordinate scale. It is clear that, unlike the constant activity for cofeed pulses, the activity of the catalyst for converting pure CH_4 pulses declined continuously with each successive pulse, even though the catalyst was calcined in O_2 for 1 h at 800°C after every tenth pulse. This result demonstrates that the deactivation caused by reaction of pure CH_4 is irreversible. Similarly, in a separate FT-IR study of this catalyst, it was observed that an initial band at 1140 cm^{-1} disappeared after exposing the catalyst to CH_4 for 1 h at 800°C or to He for 1 h at 850–900°C, and the band was not recovered completely, even after subsequent treatment in O_2 at 800°C for 16 h. The different behaviors observed for the two kinds of pulse reaction experiments suggest that there may exist two distinguishable types of sites on this catalyst, one of which is a redox site involving bulk lattice oxygen. The concentration of redox sites decreased very quickly with increased number of CH_4 pulses (corresponding to increased time on stream in the cofeed mode), and would thus make little contribution to the overall catalytic activity observed under steady-state reaction conditions. Therefore, it may be concluded that in the cofeed mode, Mn/Na catalysts, including $Mn/Na_2WO_4/SiO_2$ catalysts, are not typical redox catalysts involving bulk lattice oxygen.

Catalyst Characterization

XRD results. The phases identified by X-ray powder diffraction analyses of the various catalysts are summarized in Tables 2 and 3. The XRD results presented here can be interpreted in terms of reactions of the various components in the catalysts as follows:

$$MnO_x + Na_2WO_4 \rightleftarrows Na_2O + MnWO_4 + 0.5(x - 1)O_2 \quad [1]$$

$$MnO_x + 6MgO + 0.5(2 - x)O_2 \rightleftarrows Mg_6MnO_8. \quad [2]$$

Reaction 1 may be applied for both MgO- and SiO_2-supported catalysts, whereas, reaction 2 applies only to the former. According to the equilibrium expressed by reaction 1, it may be expected that an increase in either Mn oxide or Na_2WO_4 would result in an increase in $MnWO_4$ and Na_2O. Likewise, addition of extra Na_2O (via Na_2CO_3) to the catalyst would shift the equilibrium to the left. These trends were indeed observed in the XRD results. For the MgO-supported catalysts, either with or without Na_2WO_4, the Mg_6MnO_8 crystal phase appeared when the Mn loading was ≥0.4 wt% in the catalysts. Na_2WO_4 and $MnWO_4$ phases were detected in both the MgO- and SiO_2-supported samples when the amount of Na_2WO_4 was ≥5 wt%; Na_2WO_4 was not observed, however, when the loading was less than 5 wt%, but may have been present in a highly dispersed state (15). Both Mg_6MnO_8 and $MnWO_4$ phases increased markedly with increased amount of Mn, while the Na_2WO_4 phase correspondingly decreased. It should be mentioned that although the Mg_6MnO_8 phase was almost independent of the amount of Na_2WO_4 present in the catalysts, the $MnWO_4$ phase increased significantly as the concentration of Na_2WO_4 increased from 2 to 5 wt%. For the 5% $NaMnO_4/MgO$ catalyst, β-$Na_{0.7}MnO_2$ was formed in

TABLE 2

Bulk Phases Observed by XRD in MgO-Supported Catalysts

	MgO	Mg_6MnO_8	Na_2WO_4	$MnWO_4$	$Na_{0.7}MnO_2$	Na_2O[a]
5% Na_2WO_4/MgO	X		X			X
0.1% Mn/5% Na_2WO_4/MgO	X		X			X
0.4% Mn/5% Na_2WO_4/MgO	X	X	X	X		X
1% Mn/5% Na_2WO_4/MgO	X	X	X	X		X
2% Mn/5% Na_2WO_4/MgO	X	X	X	X		X
2% Mn/MgO	X	X				
2% Mn/2% Na_2WO_4/MgO	X	X		X		
2% Mn/10% Na_2WO_4/MgO	X	X	X	X		X
5% $NaMnO_4$/MgO	X	X			X	
Na_2CO_3/2% Mn/5% Na_2WO_4/MgO	X	X	X		X	

[a] Tentative assignment.

addition to the Mg_6MnO_8 phase. When additional Na_2CO_3 was added to the 2% Mn/5% Na_2WO_4/MgO catalyst, the β-$Na_{0.7}MnO_2$ phase also appeared, while the $MnWO_4$ phase decreased or disappeared completely.

For the SiO_2-supported catalysts containing Na_2WO_4, the dominant Mn-containing phases were $MnWO_4$ and α-Mn_2O_3. In the absence of WO_4^{2-} ions, Mn_7SiO_{12} was the only crystalline phase detected. Sodium was present in the form of sodium silicates that gave rise to a broad peak in the diffraction pattern. Addition of excess Na in the form of Na_2CO_3 to the SiO_2-supported catalyst resulted in an increase in Na_2WO_4 and SiO_2 (tridymite), but a decrease in $MnWO_4$ and SiO_2 (cristobalite).

From the results in Tables 2 and 3, it is evident that Mn exists in different crystalline forms in the various supported catalysts. Although the $MnWO_4$ phase increased upon increasing either Mn or Na_2WO_4, which correlated well with the catalytic performances shown in Fig. 4, it is probably not the active species, since no such phase was observed for the $NaMnO_4$/MgO catalyst, which displayed nearly identical catalytic behavior (Fig. 2). Similarly, β-$Na_{0.7}MnO_2$ does not play an important role in the catalytic reaction, since no such phase was observed for the samples containing WO_4^{2-} unless additional Na_2CO_3 was present. Likewise, the fact that the Mg_6MnO_8 phase was almost independent of the amount of Na_2WO_4 in the catalysts, while the C_{2+} selectivity, and consequently the CH_4 conversion, increased with increasing Na_2WO_4 content (Fig. 4b) confirms that Mg_6MnO_8 is also not the essential phase.

As suggested by the pulse reaction experiments and the XPS and ISS results (described below), a surface Mn species that is well dispersed in a Na_2CO_3/Na_2O_2/Na_2O phase may be responsible for the high activity and selectivity of these different catalysts. Therefore, it may be concluded that no single Mn phase is responsible for the high activity and C_{2+} selectivity.

XPS and ISS results. Tables 4 and 5 list the observed binding energies and near-surface compositions of selected catalysts. By comparison with their bulk compositions, the near-surface compositions of the fresh Mn/Na_2WO_4/MgO and Mn/Na_2WO_4/SiO_2 catalysts, as determined by XPS characterization, were enriched in Na and W but not in Mn. For example, the 2% Mn/5% Na_2WO_4/MgO sample had an average bulk atomic composition of 0.73% Na, 0.36% W, 0.72% Mn, and 47.6% Mg, but its surface composition was 9.6% Na, 1.9% W, 0.8% Mn, and 31% Mg. The Na/W atomic ratio of ~5 indicates that a significant amount of surface sodium was present in a form other than

TABLE 3

Bulk Phases Observed by XRD in SiO_2-Supported Catalysts

	SiO_2[a]	Na_2WO_4	$MnWO_4$	Mn_7SiO_{12}	Mn_2O_3	$Na_2Si_2O_5$[b]
2% Mn/5% Na_2WO_4/SiO_2	X	X	X		X	
2% Na_2CO_3/2% Mn/5% Na_2WO_4/SiO_2	X	X	X		X	
4% Na_2CO_3/2% Mn/5% Na_2WO_4/SiO_2	X	X	X		X	
5% $NaMnO_4$/SiO_2	X			X		X

[a] Cristobalite and tridymite.

[b] Other sodium silicates may also exist, since only a single broad peak was observed.

TABLE 4

Observed XPS Binding Energies (eV) of Catalyst Components

Catalyst	Na(1s)	W(4f)	Mn(2p)	Si(2p)	Mg(2p)	C(1s)		O(1s)	
						Advent.	CO_3^{2-}	MgO, MnO_x, WO_4^{2-}	CO_3^{2-}, silicate[c]
5% Na_2WO_4/MgO[a]	1071.2	35.7			49.5	284.6	290.9	529.6	531.7
2% Mn/5% Na_2WO_4/MgO[a]	1070.6	35.3	642.0		49.5	284.6	290.4	529.3	531.0
2% Mn/5% Na_2WO_4/MgO[b]	1070.5	35.3	641.2		49.5	284.6	290.2	529.3	530.9
2% Mn/MgO[b]	1070.7		641.3		49.5	284.6	288.2	529.5	531.2
2% Mn/2% Na_2WO_4/MgO[a]	1071.2	35.7	642.3		49.6	284.6	291.5	529.5	531.6
5% $NaMnO_4/MgO$[a]	1070.4		642.3		49.5	284.6	290.5	529.4	531.4
5% $NaMnO_4/MgO$[b]	1070.6		641.4		49.7	284.6	290.1	529.6	531.3
2% Mn/5% Na_2WO_4/SiO_2[a]	1070.3	35.1	641.0	102.8		284.6	289.6	529.5	531.6
2% Mn/5% Na_2WO_4/SiO_2[b]	1070.3	35.0	640.8	102.5		284.6	289.9	529.6	531.4
2% Na/2% Mn/5% Na_2WO_4/SiO_2[a]	1070.8	35.4	641.3	103.0		284.6	290.6	529.5	531.9

[a] Treated at 800°C in O_2 for 6–12 h after calcination at 800°C in air for 8 h.
[b] After exposure to CH_4/O_2 reaction mixture for 10 ~ 20 h at 800°C, then quenched.
[c] Silicate and silica for catalysts prepared with SiO_2.

Na_2WO_4. As shown in Table 4, a second carbon species, having a C 1s binding energy of 290 ± 1 eV, was also present on the surface of the catalyst, in addition to the adventitious carbon at 284.6 eV. This additional carbon species may be attributed to Na_2CO_3 (24), since $MgCO_3$ and $MnCO_3$ are not stable under the pretreatment conditions employed. Thus, 20–40% of the surface sodium may be in the form of Na_2CO_3. The presence of Na_2CO_3 is evidently limited to the near-surface region of the catalyst, since TPD results indicated that only small CO_2 desorption peaks, resulting from the decomposition of bulk Na_2CO_3, appeared in the temperature range 400–900°C. Thus, Na_2O_x ($x = 1 - 2$) may also be present on the surface under reaction conditions, but only a small portion of the near-surface sodium on these catalysts is in the form of Na_2WO_4. This is even more apparent in the case of the 2% Mn/2% Na_2WO_4/MgO catalyst, in which the near-surface Na/W ratio was as high as 11 (Table 5). It appears that sodium ions, which are greatly enriched on the surface, are mainly present in the form of $Na_2O/Na_2O_2/Na_2CO_3$ for the catalysts containing <5% Na_2WO_4. The presence of WO_4^{2-} ions, however, is important to the stability of

TABLE 5

Near-Surface Compositions (At.%) of Catalyst Components

Catalyst	Na(1s)	W(4f)	Mn(2p)	Si(2p)	Mg(2p)	C(1s)		O(1s)	
						Advent.	CO_3^{2-}	MgO, MnO_x, WO_4^{2-}	CO_3^{2-}, silicate[d]
5% Na_2WO_4/MgO[a]	7.9	1.4			39	0.7	1.3	42	7.5
2% Mn/5% Na_2WO_4/MgO[a]	9.6[c]	1.9	0.76		31	0.8	1.8	48	6.8
2% Mn/5% Na_2WO_4/MgO[b]	8.4	2.1	0.84		31	2.0	2.0	47	7.4
2% Mn/MgO[b]	0.9		2.1		40	3.5	2.8	44	1.7
2% Mn/2% Na_2WO_4/MgO[a]	8.5	0.9	1.6		33	0.5	1.0	47	8.0
5% $NaMnO_4/MgO$[a]	13		1.5		27	1.4	3.1	39	15
5% $NaMnO_4/MgO$[b]	6.3		2.2		29	3.9	3.2	42	13
2% Mn/5% Na_2WO_4/SiO_2[a]	10	2.4	1.7	20		1.8	1.5	24	40
2% Mn/5% Na_2WO_4/SiO_2[b]	9.9	2.6	5.0	18		3.0	2.2	23	36
2% Na/2% Mn/5% Na_2WO_4/SiO_2[a]	8.4	2.1	1.8	23		4.6	1.8	15	44

[a] Treated at 800°C in O_2 for 6–12 h after calcination at 800°C in air for 8 h.
[b] After exposure to CH_4/O_2 reaction mixture for 10 ~ 20 h at 800°C, then quenched.
[c] The percentage of Na on the surface varied between samples, but the average was about 9 at.%.
[d] Silicate and silica for catalysts prepared with SiO_2.

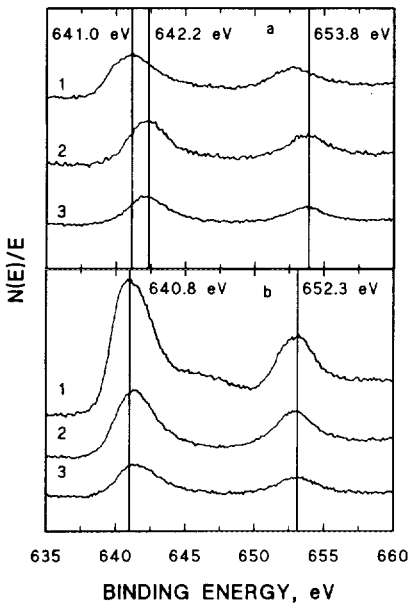

FIG. 9. XPS spectra in the Mn 2*p* region of catalysts pretreated at 800°C (a) in O_2 for 5 h and (b) in CH_4/O_2 (ratio = 10) for 20–30 h. (1) 2% Mn/5% Na_2WO_4/SiO_2; (2) 5% $NaMnO_4/MgO$; (3) 2% Mn/5% Na_2WO_4/MgO.

surface Na. As shown in Table 5, no significant change in the concentration of surface Na occurred over either the 2% Mn/5% Na_2WO_4/MgO or the 2% Mn/5% Na_2WO_4/SiO_2 catalyst after being used for the OCM reaction for 20 h; whereas, the surface Na concentration in the 5% $NaMnO_4/MgO$ catalyst decreased about 50% during the same period of reaction.

The Mn $2p_{3/2}$ binding energy in the fresh 2% Mn/5% Na_2WO_4/SiO_2 catalyst was 641.0 eV, indicating that Mn was present mainly as Mn^{3+} and Mn^{2+} (25–27). On the corresponding Mg-supported catalyst, however, Mn^{4+} predominated, since the Mn $2p_{3/2}$ binding energy in this case was 642.1 eV (28). These results are consistent with the observation that Mn exists in the form of $MnWO_4$, Mn_7SiO_{12}, or Mn_2O_3 in the SiO_2-based catalysts, whereas Mg_6MnO_8 is the major phase for the MgO-based catalysts following calcination (see above).

The chemical state of Mn in the near-surface region becomes modified under reaction conditions, however, as shown in Fig. 9. After calcination in O_2, Mn was present primarily as Mn^{3+} (BE = 641.0 eV) on the surface of the SiO_2-supported catalyst; whereas Mn^{4+} (BE = 642.2 eV) predominated on the MgO-supported catalysts, as discussed above. After exposure of the calcined sample of 2% Mn/5% Na_2WO_4/SiO_2 to an OCM reaction gas mixture (CH_4/O_2 = 10) at 800°C (the sample was quenched in He to prevent reoxidation of surface species by any unreacted O_2 during cooling), the binding energy of the Mn $2p_{3/2}$ peak decreased slightly to 640.8 eV (Fig. 9b, spectrum 1), and a small peak appeared at ~647 eV. The latter feature in the spectrum may be assigned to a $3d \rightarrow 4s$ "shake-up" satellite, which is characteristic of the Mn^{2+} oxidation state (27), indicating that at least part of the near-surface Mn^{3+} ions was reduced to Mn^{2+}. It is interesting to note that the intensities of the Mn 2*p* peaks increased after exposure to the OCM reaction mixture. An even larger change in the Mn 2*p* peaks was observed when the 2% Mn/5% Na_2WO_4/SiO_2 catalyst was reduced in pure CH_4 (not shown in Fig. 9). This change is largely reversible, since the intensities of the Mn 2*p* peaks decreased when the samples were recalcined in O_2 (29). These results suggest that a redistribution or dispersion of an Mn-containing phase may occur, since it was observed that both the Mg_6MnO_8 and the $MnWO_4$ crystalline phases disappeared after extensive reduction. It is unlikely that migration of Mn ions from the bulk to the surface occurred during reaction with CH_4 (12, 30).

Similarly, exposure of the O_2-treated 5% $NaMnO_4/MgO$ sample to the OCM reaction gas mixture at 800°C caused a slight decrease in the binding energy of the Mn $2p_{3/2}$ peak to 641.4 eV, again indicating that the surface Mn ions were partially reduced (probably to Mn^{3+} and/or Mn^{2+}) under methane coupling reaction conditions. The satellite peak, positioned at about 647 eV, was not as evident for the used 5% $NaMnO_4/MgO$ catalyst; it became more prominent, however, when the sample was reduced in pure CH_4 (29). Thus, it is apparent that Mn ions in all three catalyst samples were partially reduced upon exposure to the OCM reaction gas mixture, and the binding energies of the Mn $2p_{3/2}$ peaks were in the range 641.0 ± 0.2 eV. It appears that the chemical states of Mn species in all of these catalysts become similar under reaction conditions. These XPS results provide further evidence that the similar catalytic performances observed for these catalysts originate from the same (Mn-containing) active sites.

Although both the methane conversions and C_{2+} selectivities of these catalysts are comparable under oxygen-limited conditions (Fig. 2), it is evident from a comparison of the differential conversion data of Fig. 3 and the surface areas shown in Table 1 that the *specific* activities of these three catalysts are quite different. As depicted in Fig. 10, a linear relationship exists between the specific OCM activity and the surface Mn abundance following reaction of CH_4 and O_2. This result demonstrates that Mn ions are directly involved in the formation of the active species, probably through the activation of oxygen.

It appears that a significant amount of Mn^{3+} ions was still present on the catalysts under reaction conditions, since exposure to pure CH_4 decreased the binding energy of Mn species even further, from 641.4 to 640.5 eV, on the 5% $NaMnO_4/MgO$ catalyst (29). Based on XPS and ESR results, Mariscal *et al.* (28) concluded that Mn^{3+} is also the major Mn species in Li–Mn–MgO catalysts. It is particu-

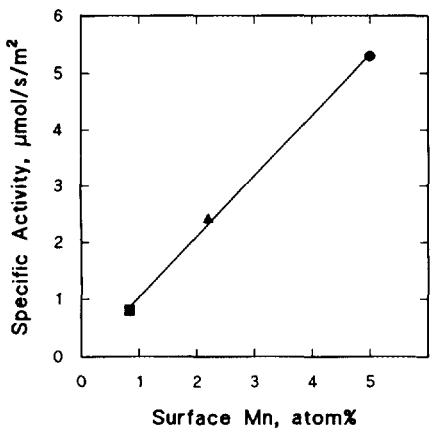

FIG. 10. Activity for oxidative coupling of methane as a function of surface Mn concentration under differential conditions (T = 800°C, CH_4/O_2 = 670/90 Torr, total flow rate = 115 ml/min, 0.3 ml catalyst). ●, 2% Mn/5% Na_2WO_4/SiO_2; ▲, 5% $NaMnO_4/MgO$; ■, 2% Mn/5% Na_2WO_4/MgO.

larly interesting to note that the Mn concentration on the 2% Mn/5% Na_2WO_4/MgO catalyst did not increase significantly after reaction, in contrast to the behavior of its SiO_2 counterpart. Mariscal *et al.* also observed that no significant changes of the surface Mn/Mg ratios occurred after their Li–Mn–MgO catalyst was reduced in H_2 (28). The different behaviors of these catalysts during the OCM reaction may reflect the fact that their bulk structures are different (29).

Interpretation of the O(1*s*) binding energies in Table 4 is somewhat complicated because of the presence of several oxygen-containing species. Oxide ions in MgO, MnO_x, and WO_4^{2-} typically have binding energies of ca. 529.5 eV. (We measured O(1*s*) BE values of 529.6 eV and 529.7 eV for MgO and Na_2WO_4, respectively; see Refs. 25–28 for BE's of MnO_x). For the catalysts based on MgO an O(1*s*) line for the carbonate ions was at a distinctly higher binding energy (~531.3 eV) than that found for the other oxygen ions, but for the catalysts based on SiO_2, O(1*s*) ambiguities may exist because silicates have an O(1*s*) binding energy of ~531.9 eV (31–35). Pure SiO_2 has an O(1*s*) binding energy of 532.5 eV (35, 36). Although carbonates were present on these catalysts, it is evident from the C(1*s*) signal (Table 5) that the oxygen in carbonates accounts for only a small fraction of the total surface oxygen in a catalyst such as 2% Mn/5% Na_2WO_4/SiO_2. Binding energies reported in Table 4 suggest that silicates were formed on the surface, but the stoichiometries of Table 5 are in better agreement with those expected for silica. In reality, a mixture of silicates and silica probably existed in the near-surface region, and differences in the O(1*s*) binding energies (~0.6 eV) were not sufficient to provide resolved spectra for these more covalent forms of oxygen.

In order to obtain additionl information about the uppermost surface layer on each of the catalysts, $^3He^+$ ISS was employed. The ISS results shown in Fig. 11 reveal that the underlying supports of all three calcined catalysts were completely covered, since no scattering peaks were observed for either Si or Mg. After sputtering the 2% Mn/5% Na_2WO_4/MgO sample with 4 keV $^{40}Ar^+$ ions for 10 min, a scattering peak for Mg appeared as a resolvable shoulder on the Na peak at an ion energy ratio of 0.66, confirming that Mg would indeed be distinguishable from Na if a significant amount of Mg were present on the surface. The surface layers of both the SiO_2- and MgO-supported catalysts contained W ions, when applicable, but only a small amount of Mn. This is more evident in the case of the 5% $NaMnO_4$/MgO catalyst, where Na^+ and O^{2-} ions were virtually the only species in the uppermost surface layer. It should be mentioned that surface carbon existed in all of the samples, although this area of the spectrum it is not included in Fig. 11. As indicated previously, W ions are not a necessary component of the active phase. These ISS results, therefore, further support the hypothesis that the similar catalytic results of Figs. 1 and 2 originate from the same active species, which consists of an Na–O–Mn entity.

In contrast to the nature of many other effective OCM catalysts, the active surfaces of these Mn-containing catalysts are not highly basic, since CO_2 TPD studies revealed no evidence for a significant amount of strongly adsorbed CO_2. Apparently, the basicity of the Na_2O was altered by the lower basicity of other components in the catalysts (37). The XPS results, however, indicate that a moderate amount of carbonate exists, presumably as only a thin surface layer, but only a slight CO_2 poisoning effect was

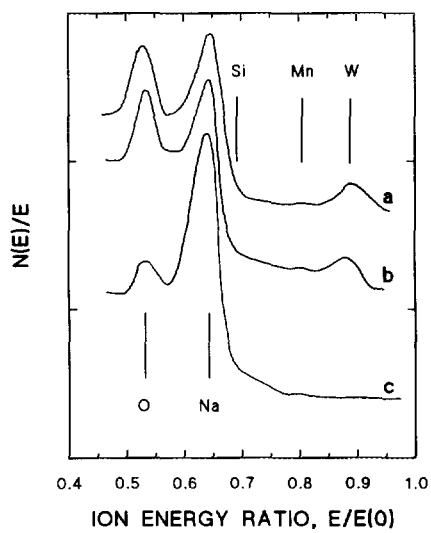

FIG. 11. Ion scattering spectra of fresh catalysts. (a) 2% Mn/5% Na_2WO_4/SiO_2; (b) 2% Mn/5% Na_2WO_4/MgO; (c) 5% $NaMnO_4$/MgO. The samples were pretreated at 800°C in O_2 for 8 h.

observed for these catalysts, including the 5% Na_2CO_3/MgO material. When the CO_2 partial pressure was increased, for example, from about 5 to 50 Torr, the methane conversion over the 2% Mn/5% Na_2WO_4/SiO_2 catalyst only decreased from 5.5 to 4.8%, while the selectivity remained virtually constant.

Nature of the Active Sites

The exact nature of the catalytically active sites on these materials has not been unambiguously determined; however, it is clear that small concentrations of Mn play an essential role in achieving high activities and selectivities, and that Na is also a required component particularly for achieving good selectivities. The role of sodium ions, which dominate the near-surface region of the catalyst, may be to disperse the Mn ions. From the results shown in Table 5, it is clear that the surface Mn concentration decreases as the Na content increases, indicating that Na ions promote diffusion of Mn ions into the MgO bulk (29). Since ethylene is a major source of CO_2 during oxidative coupling (38), the undesirable π bonding of ethylene to the surface may be minimized if the Mn ions are highly dispersed.

Manganese may exist in several oxidation states, having varying degrees of interconversion under reaction conditions; therefore, it is difficult to establish which, if any, of these chemical states may be responsible for promoting the high activity/selectivity behaviors of these catalysts. From the results in Figs. 4 and 7, it is evident that the Na-free Mn/MgO catalyst, in which Mg_6MnO_8 was the only detectable Mn phase, was inferior in catalytic performance. Therefore, Mn^{4+} ions are probably not the selective active species for the methane coupling reaction. A similarly poor result was previously observed over Mg_6MnO_8 catalysts in the cofeed mode (39), although it was still proposed that Mg_6MnO_8 may be the active phase (12). Based on the XPS data for the used catalysts, which were quenched in a He stream, the Mn ions are present as Mn^{3+} and/or Mn^{2+}, suggesting that these partially reduced Mn ions may form the active species. Burch *et al.* (13) concluded, based on information obtained from XRD experiments, that none of the various pure manganese oxides were selective phases, whereas an Mn_3O_4-like phase, promoted by K and in the presence of Cl, was highly selective. However, it should be emphasized that the active species on these Mn/Na catalysts were generated when the sodium-dominated surface was exposed to O_2, and had a short lifetime under reaction conditions. Therefore, it is unlikely that these stable phases function as active species in the catalysts studied here.

CONCLUSIONS

Based on CH_4 conversion and C_{2+} selectivity, as well as on long-term stability and performance at higher pressures, Mn/Na_2WO_4/MgO and Mn/Na_2WO_4/SiO_2 catalysts rank among the best that have yet been reported for the oxidative coupling of methane. The active component is believed to be Mn in a highly dispersed state. Sodium is required for high selectivity, and it is suggested that individual Mn ions are present in a $Na_2O/Na_2O_2/Na_2CO_3$ surface phase. Tungstate ions are required to stabilize the catalysts. The active center is a transient state that exists only in the presence of gas-phase O_2. Thus, it seems unlikely that lattice oxygen in the bulk of the catalysts is involved in the catalytic reaction. Although several crystalline phases are present, none appears to be directly associated with the catalytic performance. These phases, however, may be indirectly involved by influencing the concentration and oxidation state of Mn on the surface.

ACKNOWLEDGMENT

This research was supported by the Gas Research Institute under Contract 5086-260-1326 and by the National Science Foundation under Grant CHE 9005808

REFERENCES

1. Renesme, G., Saint-Just, J., and Muller, Y., *Catal. Today* **13,** 371 (1992).
2. Wolf, E. E., Ed., "Methane Conversion by Oxidative Processes." Van Nostrand–Reinhold, New York, 1992.
3. Lunsford, J. H., *in* "Proceedings, 10th International Congress on Catalysis, Budapest, 1992" (L. Guezi, F. Solymosi, and P. Tetenyi, Eds.), p. 103. Akadémiai Kiadó, Budapest, 1993.
4. Mimoun, H., Robine, A., Bonnaudet, S., and Cameron, C. J., *Chem. Lett.*, 2185 (1989).
5. Ruckenstein, E., and Khan, A. Z., *Catal. Lett.* **18,** 27 (1993).
6. Dissanayake, D., Doctoral dissertation, Texas A & M University, 1993.
7. Sofranko, J. A., Leonard, J. J., Jones, C. A., Gaffney, M. M., and Witheres, J. A., *Catal. Today* **3,** 127 (1988).
8. Fang, X., Li, S., Lin, J., Gu, J., and Yang, D., *J. Mol. Catal.* (China) **6,** 427 (1992).
9. Khan, A. Z., and Ruckenstein, E., *J. Catal.* **138,** 322 (1992).
10. Sofranko, J. A., Leonard, J. J., and Jones, C. A., *J. Catal.* **103,** 302 (1987).
11. Jones, C. A., Leonard, J. J., and Sofranko, J. A., *J. Catal.* **103,** 311 (1987).
12. Labinger, J. A., Ott, K. C., Mehta, S., Rockstad, H. K., and Zoumalan, S., *J. Chem. Soc. Chem. Commun.*, 543 (1987).
13. Burch, R., Chalker, S., Squire, G. D., and Tsang, S. C., *J. Chem. Soc. Faraday Trans.* **86,** 1607 (1990).
14. Moggridge, G. D., Rayment, T., and Lambert, R. M., *J. Catal.* **134,** 242 (1992).
15. Jiang, Z., Yu, C., Fang, X., Li, S., and Wang, H., *J. Phys. Chem.* **97,** 12870 (1993).
16. Keller, G.E., and Bhasin, M. M., *J. Catal.* **73,** 9 (1982).
17. Otsuka, K., Liu, Q., Hatano, M., and Mariawa, A., *Chem. Lett.*, 486 (1986).
18. Hatano, M., and Otsuka, K., *Inorg. Chim. Acta.* **146,** 243 (1988).
19. Otsuka, K., Hatano, M., and Komatsu, T., *Catal. Today* **4,** 409 (1989).
20. Miro, E., Santamaria, J., and Wolf, E. E., *J. Catal.* **124,** 451 (1990).

21. Gaffney, A. M., Jones, C. A., Leonard, J. J., and Sofranko, J. A., *J. Catal.* **114,** 422 (1988).
22. Tong, Y., Rosynek, M. P., and Lunsford, J. H., *J. Phys. Chem.* **93,** 2896 (1989).
23. Pinabian-Carlier, M., Ben Hadid, A., and Cameron, C. J., *in* "Natural Gas Conversion" (A. Holmen, K.-J. Jens, and S. Kolboe, Eds.), pp. 183–190. Elsevier, Amsterdam, 1991.
24. Hammond, J. S., Holubka, J. W., Devries, J. E., and Duckie, R. A., *Corros. Sci.* **21,** 239 (1981).
25. Judd, R. W., Komodromos, C., and Reynolds, T. J., *Catal. Today* **13,** 237 (1992).
26. Strohmeier, B. R., and Hercules, D. M., *J. Phys. Chem.* **88,** 4922 (1984).
27. Oku, M., Hirokawa, K., and Ikeda, S., *J. Electron Spectrosc. Relat. Phenom.* **7,** 465 (1975).
28. Mariscal, R., Soria, J., Pena, M. A., and Fierro, J. L. G., *J. Catal.* **147,** 535 (1994).
29. Wang, D., Rosynek, M. P., and Lunsford, J. H., manuscript in preparation.
30. Cordischi, D., Nelson, R. L., and Tench, A. J., *Trans. Faraday Soc.* **65,** 2740 (1969).
31. Clarke, T. A., and Rizkalla, E. N., *Chem. Phys. Lett.* **37,** 523 (1976).
32. Lorenz, P., Finster, J., Wendt, G., Salyn, J. V., Zumadilov, E. K., and Nefedov, V., *J. Electron Spectrosc. Relat. Phenom.* **16,** 267 (1979).
33. Wagner, C. D., Zatko, D. A., and Raymond, R. H., *Anal. Chem.* **52,** 1445 (1980).
34. Anderson, P. R., and Swartz, W. E., *Inorg. Chem.* **13,** 2293 (1974).
35. Wagner, C. D., Passoja, D. E., Hillery, H. F., Kinisky, T. G., Six, H. A., Jansen, W. T., and Taylor, J. A., *J. Vac. Sci. Technol.* **21,** 933 (1982).
36. Shalvoy, R. B., Reucroft, P. J., and Davis, B. H., *J. Catal.* **56,** 336 (1979).
37. Dissanayake, D., Lunsford, J. H., and Rosynek, M. P., *J. Catal.* **143,** 286 (1993).
38. Shi, C., Rosynek, M. P., and Lunsford, J. H., *J. Phys. Chem.* **98,** 8371 (1994).
39. Chan, T. K., and Smith, K. J., *Appl. Catal.* **60,** 13 (1990).